



# Investigation on the effect of supplementary cementitious materials on the critical chloride threshold of steel in concrete

Federica Lollini · Elena Redaelli · Luca Bertolini

Received: 13 May 2015 / Accepted: 21 December 2015 / Published online: 24 December 2015  
© RILEM 2015

**Abstract** The critical chloride threshold is a key parameter in the service life design of reinforced concrete structures exposed to chloride-bearing environments. This paper investigates the role of concrete composition, and particularly the effect of supplementary cementing materials, on the chloride threshold. To simulate real exposure conditions, ponding tests were carried out on reinforced concrete specimens with bars in free corrosion conditions and corrosion initiation was detected through corrosion potential and corrosion rate measurements. After two and a half years, the ponding was followed by an ageing period and the initiation of corrosion was further detected with anodic potentiostatic polarisation tests. Results of the tests showed several limitations of the approach based on chloride penetration and monitoring of free corrosion parameters to investigate the chloride threshold. In spite of this, a possible role of natural pozzolan and coal fly ash additions in leading to higher values of the chloride threshold and ground limestone in promoting lower values of the chloride threshold could be observed.

**Keywords** Chloride · Concrete · Corrosion · Blended cement · Ponding tests · Potentiostatic tests

---

F. Lollini (✉) · E. Redaelli · L. Bertolini  
Department of Chemistry, Materials and Chemical Engineering “Giulio Natta”, Politecnico di Milano,  
Piazza Leonardo da Vinci 32, 20133 Milan, Italy  
e-mail: federica.lollini@polimi.it

## 1 Introduction

A reliable estimation of the chloride threshold ( $Cl_{th}$ ) is a fundamental step in the prediction of the service life of reinforced concrete (RC) structures exposed to marine environments or the action of de-icing salts [10, 15, 55]. In the literature, several test methods have been proposed to evaluate the critical chloride threshold. Limiting to the tests in concrete, which are expected to be intrinsically more realistic compared to tests in solution, methods proposed by different Authors differ regarding the way concrete is contaminated by chloride ions, corrosion initiation is detected and the chloride content at the depth of the bar is measured. Chlorides can be forced to penetrate into concrete through external sources [8, 19, 20, 22, 24, 25, 29, 31, 32, 38, 40, 45–47, 50, 52–54, 56, 57], as for instance ponding with chloride-containing solutions [32, 46], or alternatively can be added to the concrete mix [2, 30, 32, 35, 39, 41, 47]. The way chlorides are introduced into concrete has several consequences. Tests with chlorides which penetrate from an external source can have excessively long duration, although they are often assumed to better simulate exposure of real structures to marine environments or de-icing salts. Conversely tests with mixed-in chlorides are relatively short, but the microstructure of the interfacial transition zone between steel bar and concrete, as well as the passivation of steel, can be affected by the presence of chloride ions since the early stage of hydration.



The initiation of corrosion is often detected by non-destructive monitoring of electrochemical parameters (e.g. corrosion potential and corrosion rate) [2, 8, 19, 25, 29, 32, 35, 38, 40, 41, 46, 56] and, seldom, by extraction of bars and visual inspection [20] or weight loss [52, 53]. As far as the measurement of the chloride content is concerned, the analysis of total chloride content is frequently applied in practice. Different criteria for sampling have been proposed: directly from the bar site at the time of corrosion onset [3, 19, 28, 31, 41, 50, 54, 57] or far from the bar considering the same bar depth [25, 39, 40, 45, 52, 53] (sometimes even in reference samples exposed to the same exposure conditions, provided similar conditions for chloride penetration occur [38]). Tests can also be different for other aspects such as, for instance, the bar surface conditions, the specimen geometry, etc.

Differences in the test procedures used by different Authors is one of the reasons that may lead to a great variation in the values of the critical chloride threshold published in the literature [4, 7, 9, 27, 48]. This makes the comparison of results of different works quite difficult and, consequently, hinders the evaluation of the role of factors that influence the critical chloride threshold.

Nowadays there is a great interest in studying a possible influence of the binder type (and concrete composition, in general) on the critical chloride threshold, due to the availability of a great variety of supplementary cementing materials (SCMs), as also underlined by the activity of specific technical committees (e.g. RILEM TC 235-CTC, [www.rilem.org](http://www.rilem.org)). As a matter of fact, the type of binder may affect the chloride threshold in several ways. It influences the alkalinity of the pore solution, the availability of free chlorides in the pore solution as a result of chloride binding, the electrical resistivity of concrete or the microstructure of the steel–concrete interface.

Even though the evaluation of the effect of SCMs on the critical chloride threshold has received some interest in the literature, the results are often controversial. For instance, Thomas and Matthews [53], Oh et al. [41] and also Song et al. [49] reported a reduction in the critical chloride threshold of fly ash (FA) concrete compared to portland cement (OPC) concrete. Conversely, according to Breit and Schiessl [17] and Choi et al. [21], the critical chloride threshold for FA concrete was higher than for portland cement. Alonso et al. [3] did not find significant differences in

the critical chloride threshold when portland cement was partially replaced with fly ash. Controversial results were also obtained with the replacement of ground granulated blast furnace slag (GGBS): Oh et al. [41] observed a negligible influence of GGBS on the critical chloride threshold, while Breit and Schiessl [17] reported a higher critical chloride threshold for GGBS concrete.

This work describes the results of a study aimed at the assessment of the critical chloride threshold of bars embedded in twenty-six concrete mixes made with various types of binder. To simulate real exposure conditions, long-term tests were carried out with penetration of chloride ions through ponding and bars in free corrosion conditions.

## 2 Experimental procedure

Binders were obtained by blending a portland cement (OPC) with 15 % (15 %LI) and 30 % (30 %LI) ground limestone, 30 % coal fly ash (30 %FA), 30 % natural pozzolan (30 %PZ), and 70 % GGBS (70 %BF). The chemical composition and the specific surface area of OPC and additions are shown in Table 1. These binders were used to cast concrete with three water/binder ratios (0.42, 0.46 and 0.61), and four binder dosages, ranging from 250 to 400 kg/m<sup>3</sup>. Crushed limestone aggregate with maximum size of 12.5 mm was used. An acrylic high-range water-reducing superplasticiser (according to EN 934-2 Standard) was added to the mixes in order to achieve a class of consistency S4 according to EN 206 Standard. Table 2 summarises the concrete mix proportions. After mixing, concrete was cast into the moulds, covered with a plastic sheet and stored in laboratory at 20 °C. After 24 h, the specimens were demoulded and cured until 7 or 28 days at 20 °C and 95 % relative humidity. In the text, specimens will be indicated by the label “type of binder/w/b ratio/binder dosage/curing time” (CL1 and CL2 indicate replicate specimens cured 7 days; CL3 indicates 28-day curing).

100 mm cubes were cast for the measurement of compressive strength (two replicate cubes) and results obtained after 28 days of curing are shown in Table 2 (further results can be found in [34]). 64 prism specimens, 60 mm × 250 mm × 150 mm, reinforced with ribbed carbon steel bars with a diameter

**Table 1** Main chemical components and specific surface area,  $\sigma$ , of portland cement and mineral additions

	CaO (%)	SiO <sub>2</sub> (%)	Al <sub>2</sub> O <sub>3</sub> (%)	SO <sub>3</sub> (%)	Fe <sub>2</sub> O <sub>3</sub> (%)	MgO (%)	K <sub>2</sub> O (%)	Na <sub>2</sub> O (%)	Mn <sub>2</sub> O <sub>3</sub> (%)	TiO <sub>2</sub> (%)	Cl <sup>-</sup> (%)	$\sigma$ (cm <sup>2</sup> /g)
OPC	63.5	20.5	5.28	3.29	2.84	1.53	1.0	0.29	0.07	0.24	0.01	5340
LI	43.8	15.8	1.98	0.27	0.80	1.10	0.6	0.06	0.05	0.11	–	6102
FA	2.92	52.9	33.2	0.73	5.23	1.06	1.2	0.72	0.04	1.17	–	5437
PZ	4.49	54.6	21.1	0.14	4.4	1.19	7.0	3.52	0.15	0.55	0.01	4606
BF	41.7	33.9	13.0	2.10	0.37	6.62	0.3	0.45	0.24	0.54	0.257 <sup>a</sup>	5624

<sup>a</sup> This amount corresponds to 0.18 % with respect to the mass of binder, since BF cement was made with 70 % of ground granulated blast furnace slag

**Table 2** Mix proportions of concrete and average value of compressive strength on cubes after 28 days of curing,  $f_{c,cube,28}$ 

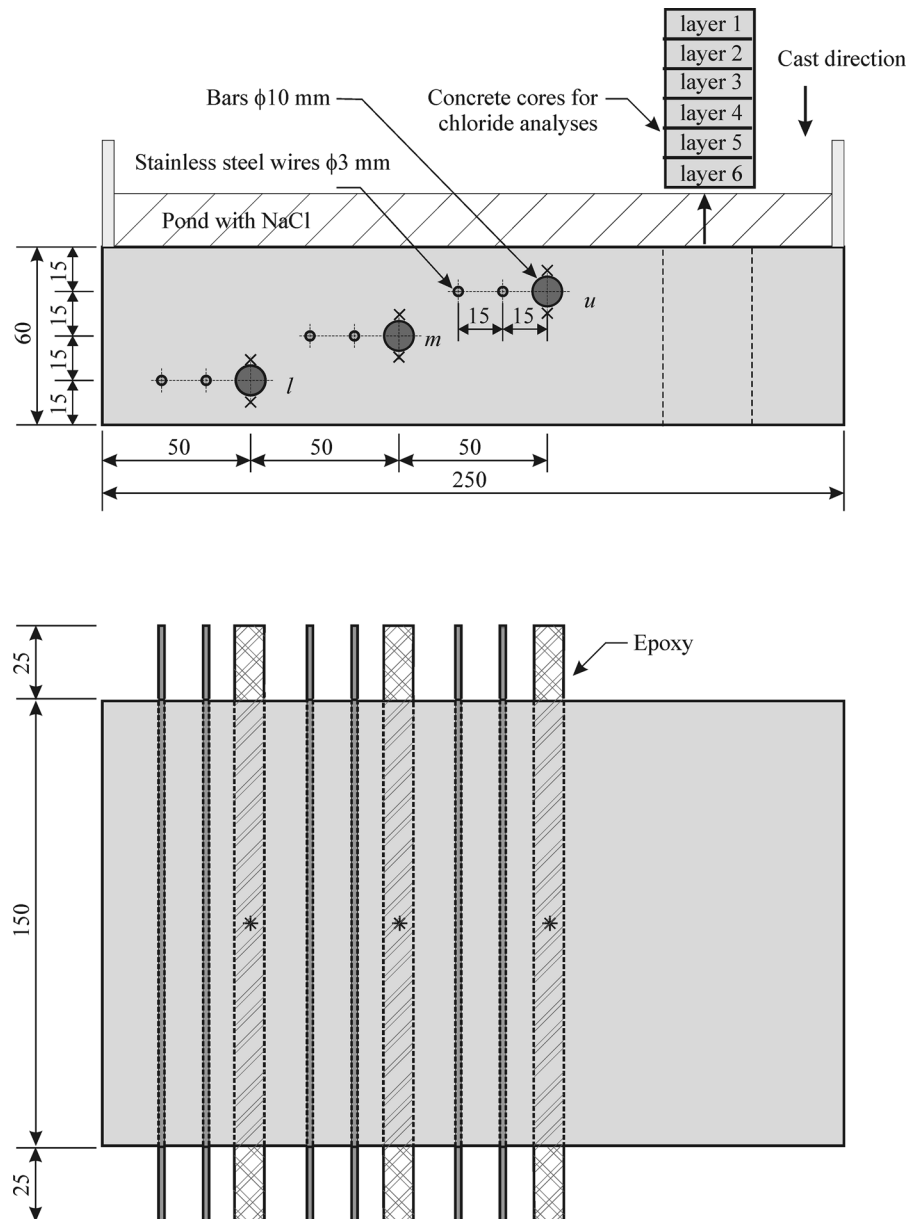
Type of binder	w/b	Binder (kg/m <sup>3</sup> )	Water (kg/m <sup>3</sup> )	Aggregate (kg/m <sup>3</sup> )	$f_{c,cube,28}$ (MPa)
OPC	0.61	300	183	1857	59
	0.46	300	138	1979	87
	0.46	350	161	1868	80
	0.42	350	147	1913	87
15 %LI	0.61	250	152	1983	55
	0.61	300	183	1857	45
	0.46	300	138	1979	75
	0.46	350	161	1868	68
30 %LI	0.42	350	147	1913	83
	0.42	400	168	1815	68
	0.61	300	183	1857	37
	0.46	300	138	1979	61
30 %FA	0.46	350	161	1868	57
	0.42	350	147	1913	67
	0.61	300	183	1857	44
	0.46	300	138	1979	76
30 %PZ	0.46	350	161	1868	75
	0.42	350	147	1913	81
	0.61	300	183	1857	43
	0.46	300	138	1979	70
70 %BF	0.46	350	161	1868	69
	0.42	350	147	1913	73
	0.61	300	183	1857	45
	0.46	300	138	1979	55
	0.46	350	161	1868	55
	0.42	350	147	1913	83

of 10 mm and a length of 200 mm, were cast. Before casting the bars were sandblasted in order that the bars had the same surface condition. Each specimen had three rebars at different cover depths (i.e. concrete

cover thickness was 10, 25 and 40 mm respectively for the upper (*u*), middle (*m*) and lower (*l*) bar) and stainless steel wires were used as auxiliary electrodes for electrochemical measurements (Fig. 1). The



**Fig. 1** Geometry of reinforced concrete specimen (dimensions in mm) (plan view and cross-section) with indication of sampling for chloride analyses through coring. Symbols *times* indicate location of powders manually ground near each bar site. Symbols *asterisk* indicate the position of the electrode during the potential measurements



lateral surface of the specimens as well as the external parts of the rebars were masked with an epoxy coating. After 90 days from casting, a pond was mounted on the upper surface of the specimen and a 35 g/l sodium chloride solution was poured inside (evaporation of water was allowed from the bottom surface of the specimens). The corrosion behaviour of steel was monitored throughout an exposure period of more than 2 years by means of electrochemical measurement of half-cell potential of steel ( $E_{\text{corr}}$ ) versus a saturated calomel electrode (SCE), placed on the specimen

surface in the central part of each bar, and corrosion current density, measured through linear polarisation resistance measurements ( $R_p$ ) as:  $v_{\text{corr}} = B/(R_p)$ , where  $B$  was assumed equal to 26 mV. Electrochemical measurements were carried out daily in the first month of exposure and then weekly and monthly. During the measurements the pond was not removed.

When corrosion initiation was detected on any of the three rebars, a sample was cored in the lateral non-reinforced part of the specimen and the chloride profile was measured by analysing the total chloride content

(acid soluble) at intervals of 10 mm, as shown in Fig. 1. Known the nominal binder content (Table 2) and the concrete density measured on the cubes for compressive strength, the chloride content was expressed by mass of binder. The chloride profiles were fitted with the relationship:

$$C(x,t) = C_0 + (C_s - C_0) \cdot \left[ 1 - \operatorname{erf} \left( \frac{x}{\sqrt{D_{app} \cdot t}} \right) \right] \quad (1)$$

and the apparent diffusion coefficient,  $D_{app}$  and the surface content,  $C_s$  were calculated (the initial chloride content,  $C_0$ , was considered 0 % except for concrete with BF where 0.18 % by mass of binder was considered, see Table 1). The specimens were then exposed to ponding again (the hole of coring was filled with epoxy). Additional coring for the determination of the chloride profile was carried out after the interruption of the ponding exposure on all the specimens regardless the occurrence of corrosion.

After the interruption of ponding, the specimens were kept in dry conditions, i.e. in the lab at 20–23 °C and 60–65 % R.H. (ageing phase), for approximately 1 year, and then they were wetted again through a ponding with tap water for approximately 1 month, during which the electrochemical behaviour of bars was monitored (the ageing phase was not performed on OPC concrete specimens). Afterwards, selected specimens were cut parallel to the bars to obtain three samples with a single bar each and the extremities of these samples (approximately 15 mm on each side) were cut and masked with an alkaline mortar with a thickness of 20–30 mm (carbonation depth was nil) (no OPC samples were tested). These samples were then immersed individually in a container filled with a saturated  $\text{Ca}(\text{OH})_2$  solution and kept in a climatic chamber at 23 °C. In each container a silver/silver chloride ( $\text{Ag}/\text{AgCl}$ ) reference electrode and an activated titanium mesh for cathodic protection, to be used as counter-electrode, were placed. After a 24-hour period of immersion, the corrosion potential and the corrosion current density were measured and then the potential was increased by steps of +50 mV per hour, monitoring the circulating current (potentiostatic tests). The polarisation was interrupted when the circulating current exceeded 100 mA/m<sup>2</sup> or when the potential reached +600 mV versus SCE.

Specimens with bars where corrosion had initiated during the ponding tests and specimens subjected to polarisation tests were split to extract the bars and the steel surface was visually observed. Furthermore, concrete dust was manually ground within a depth of 1–2 mm near the top and bottom bar sites (Fig. 1) and the total chloride content was analysed.

### 3 Results

Ninety days after casting, the monitoring of the corrosion potential ( $E_{\text{corr}}$ ) and the corrosion rate ( $v_{\text{corr}}$ ) of the bars started. As expected, all the bars were in passive conditions: the corrosion potential was between –150 and 100 mV vs SCE, whilst the corrosion rate was lower than 1 mA/m<sup>2</sup>, regardless the concrete composition, the curing time and the concrete cover thickness. The upper bar of specimen 70 %BF/0.61/300/CL2 was the only exception, since  $E_{\text{corr}}$  was lower than –400 mV versus SCE and  $v_{\text{corr}}$  was around 4 mA/m<sup>2</sup>. It seems that chlorides present in the slag (0.18 % by mass of binder, Table 1) were enough to initiate corrosion of this bar.

#### 3.1 Ponding

All the specimens were subjected to ponding with a 3.5 % NaCl solution. Results of these tests are summarized in Tables 3, 4, and 5. By monitoring  $E_{\text{corr}}$  and  $v_{\text{corr}}$ , four different cases were detected, which are shown in the examples of Fig. 2. Figure 2a depicts the time evolution of the corrosion potential and the corrosion rate of the middle bar of specimen OPC/0.61/300/CL2: in this case, stable values of  $E_{\text{corr}}$  and  $v_{\text{corr}}$ , respectively around –100 mV versus SCE and 0.5 mA/m<sup>2</sup>, were measured throughout the exposure period, showing the maintenance of the passive state in spite of chloride penetration. This stable passive condition was observed on 133 out of 192 rebars, i.e. approximately 70 % of the total bars (these bars are indicated as *P* in Table 3). In Fig. 2b, the behaviour of the upper bar of the same specimen is reported. After 121 days of ponding the potential sharply dropped to about –350 mV vs SCE and the corrosion rate increased to about 3 mA/m<sup>2</sup>. A further decrease of  $E_{\text{corr}}$  and an increase of  $v_{\text{corr}}$  occurred in time. The sudden drop in  $E_{\text{corr}}$  together with a significant increase of  $v_{\text{corr}}$  clearly identified the onset

**Table 3** Results of ponding tests on upper **u**, middle **m**, and lower **l**, bars: for active bars = time (in days) when corrosion initiated (bold cells); P = passive bar; U bars with unstable condition; ? = unclear case

Binder	<i>w/b</i>	Series curing (days)	CL1			CL2			CL3		
			7			7			28		
			<i>u</i>	<i>m</i>	<i>l</i>	<i>u</i>	<i>m</i>	<i>l</i>	<i>u</i>	<i>m</i>	<i>l</i>
OPC	0.61	300		–		<b>121</b>	P	P		–	
	0.46	300	U	P	U	U	P	U	P	P	P
	0.46	350	P	U	U	P	P	P	P	P	P
	0.42	350	P	P	P	U	P	P	P	P	P
15 %LI	0.61	250		–		<b>14</b>	<b>313</b>	<b>341</b>		–	
	0.61	300		–		<b>13</b>	<b>106</b>	<b>854</b>		–	
	0.46	300	U	P	U <sup>a</sup>	U	P	U	?	P	U <sup>a</sup>
	0.46	350	P	P	U	U + ? <sup>b</sup>	P	P	U <sup>a</sup>	U	U
	0.42	350	P	P	P	P	P	P	P	P	P
	0.42	400	P	P	P	U + ?	P	P	P	P	U
30 %LI	0.61	300		–		<b>7</b>	<b>140</b>	<b>276</b>		–	
	0.46	300	U <sup>a</sup>	P	U <sup>a</sup>	U	P	U <sup>a</sup>	<b>229</b>	P	P
	0.46	350	<b>27</b>	U + ? <sup>b</sup>	U	<b>89</b>	? <sup>b</sup>	U	U	P	U <sup>a</sup>
	0.42	350	P	P	P	P	P	U	U <sup>a</sup>	P	P
30 %FA	0.61	300		–		<b>359</b>	P	U		–	
	0.46	300	P	P	U <sup>a</sup>	P	P	P	P	P	P
	0.46	350	U <sup>a</sup>	P	P	U <sup>a</sup>	P	P	U	P	P
	0.42	350	U <sup>a</sup>	P	P	P	P	P	P	P	P
30 %PZ	0.61	300		–		<b>54</b>	P	U <sup>a</sup>		–	
	0.46	300	P	P	P	P	P	P	U	P	P
	0.46	350	P	P	P	U <sup>a</sup>	P	P	P	P	P
	0.42	350	P	P	P	P	P	P	P	P	P
70 %BF	0.61	300		–		<0 <sup>c</sup>	P	P		–	
	0.46	300	P	P	P	? <sup>b</sup>	P	P	U	P	P
	0.46	350	P	P	P	P	P	P	P	P	P
	0.42	350	P	P	P	P	P	P	P	P	P

– = absence of specimen

<sup>a</sup> At the end of ponding exposure the corrosion potential was lower than the corrosion potential at the beginning of the exposure

<sup>b</sup> Ponding test was interrupted before detecting a clear trend

<sup>c</sup> Corrosion occurred before the initiation of ponding exposure

of corrosion on this bar after 3 months. Initiation of corrosion, after different times of exposure ranging from few days to 2 years and an half, was observed on only 15 bars (less than 10 % of the total number of rebars). These bars are shown in Table 4. Considering only the upper bars of the specimens (*u*, 10 mm cover thickness), corrosion occurred on 1 out of 10 rebars embedded in OPC, 30 %FA and 30 %PZ concretes, 2 out of 14 rebars in 15 %LI concrete and 4 out of 10 rebars in 30 %LI concrete (Table 3). In these bars the drop in  $E_{\text{corr}}$  and the associated increase in  $v_{\text{corr}}$ , occurred in a period of time ranging from few days up to 2 weeks.  $E_{\text{corr}}$  values measured before corrosion initiation are shown in Table 4.

The third case is illustrated in Fig. 2c (upper bar of specimen OPC/0.42/350/CL2): after 90 days,  $E_{\text{corr}}$

decreased to about -350 mV versus SCE and  $v_{\text{corr}}$  increased to 2.5 mA/m<sup>2</sup>. However, few days afterwards this trend was reversed and both  $E_{\text{corr}}$  and  $v_{\text{corr}}$  returned to the initial values after about 100 days. This behaviour, that suggests that the passive state was unstable for some time but then stable passive conditions were recovered, was observed on 40 bars (i.e. about 20 % of the total tested bars), as it can be seen in Table 3. In few specimens, this phenomenon occurred even twice during the ponding exposure time. Finally, Fig. 2d shows results for the upper bar of the specimen 15 %LI/0.46/300/CL3. After about 470 days from the beginning of the exposure, the corrosion potential of the bar abruptly decreased by about 200 mV, approaching values of -200 mV versus SCE. Except some oscillations, the potential was thereafter stable,



**Table 4** Summary of results on the 15 bars which showed corrosion initiation during the ponding phase

Binder	$w/b$	$b$ (kg/m <sup>3</sup> )	Series	Bar	$E_{\text{corr}}^{\text{a}}$	$Cl_{\text{cores}}^{\text{b}}$					$Cl_{\text{grind}}^{\text{c}}$		V.O. <sup>d</sup>	
						$C_s$	$D_{\text{app}}$	$Cl_{\text{top}}$	$Cl_{\text{ave}}$	$Cl_{\text{bot}}$	Top	Bottom	Top	Bottom
OPC	0.61	300	CL2	u	−101	2.82	16.7	1.78	1.32	0.95	5.67	2.11	✓✓	✓✓
15 %LI	0.61	250	CL2	u	−107	2.34	49.35	0.98	0.53	0.25	3.00	2.38	✓✓	✓✓
				m	−65	2.28	33.5	1.25	1.07	0.91	2.51	3.56	–	✓
				l	−102	3.77	12.5	0.48	0.32	0.21	4.14	1.81	✓	–
15 %LI	0.61	300	CL2	u	−91	2.06	35.5	0.54	0.19	0.05	1.90	2.27	✓✓	✓✓
				m	−104	2.47	20.9	0.50	0.31	0.18	2.37	3.92	✓✓	✓
				l	−84	6.14	16.4	0.87	0.63	0.44	3.62	1.97	✓	✓
30 %LI	0.61	300	CL2	u	−56	1.01	166	0.56	0.38	0.24	7.30	7.77	✓✓	✓✓
				m	−65	3.80	28.3	1.32	0.99	0.72	4.96	3.81	✓✓	✓✓
				l	−79	3.4	27.8	0.77	0.59	0.44	2.38	0.43	✓	✓
30 %LI	0.46	300	CL3	u	−52	1.81	12.5	1.18	0.91	0.67	2.29	1.90	✓✓	✓
30 %LI	0.46	350	CL1	u	−65	0.93	134.2	0.67	0.55	0.44	2.40	2.16	✓✓	✓✓
30 %LI	0.46	350	CL2	u	−63	1.88	35.1	1.23	0.94	0.70	2.20	2.48	✓✓	✓
30 %FA	0.61	300	CL2	u	−51	2.20	21.94	3.32	1.89	0.96	4.85	1.88	✓✓	✓
30 %PZ	0.61	300	CL2	u	−91	2.20	21.94	1.06	0.64	0.35	4.64	4.06	✓✓	✓

<sup>a</sup> Corrosion potential before the occurrence of corrosion,  $E_{\text{corr}}$  (mV vs SCE)

<sup>b</sup> Results of chloride profiles measured soon after detection of corrosion initiation on the bars: chloride surface concentration,  $C_s$  (% vs binder), diffusion coefficient,  $D_{\text{app}}$  ( $10^{-12}$  m<sup>2</sup>/s), and chloride content (% vs binder) calculated at top,  $Cl_{\text{top}}$ , average,  $Cl_{\text{ave}}$ , and bottom,  $Cl_{\text{bot}}$ , depths of the bars

<sup>c</sup> Chloride content measured by grinding in the vicinity of the top and bottom part of the bar after the specimens breaking

<sup>d</sup> Visual observation – = no sign of corrosion; ✓ = low level of corrosion (was localised in a limited area); ✓✓ = high level of corrosion (corrosion was present on the whole surface of the bars or a broad portion of the surface)

but no appreciable increase in the corrosion rate could be detected. This undefined behaviour was observed on 7 bars (<5 % of the total number of bars).

In order to describe the ranges of variation of corrosion potential and corrosion rate during the ponding phase, Fig. 3 shows the relationship between  $E_{\text{corr}}$  and  $v_{\text{corr}}$  for the three rebars of each specimen. Values measured on all the bars at the end of ponding exposure are reported; furthermore, for those bars where corrosion initiated, values at the end of the transition period between passive/active state are reported and, for bars which experienced unstable passive conditions, the peaks reached in the unstable period are shown. At the end of ponding exposure (empty symbols), the passivity of most of the bars is shown by corrosion potential between −150 and +50 mV versus SCE and corrosion rate lower than 1 mA/m<sup>2</sup>. On bars where corrosion initiated,  $E_{\text{corr}}$  values lower than −250 mV versus SCE and  $v_{\text{corr}}$  values higher

than 1 mA/m<sup>2</sup> were measured after the transition from passive to active state (black symbols), regardless the type of cement, the water/binder ratio, curing time and concrete cover thickness. The typical linear relationship between  $E_{\text{corr}}$  and  $\log(v_{\text{corr}})$  was observed [1, 26]. Also values measured during the unstable initiation condition, observed on some bars (grey symbols), followed this relationship.

In order to measure the chloride content as close as possible to the time of initiation, chloride profiles were measured in the non-reinforced part of specimens when a bar showed a drop in  $E_{\text{corr}}$  below −250 mV versus SCE or an increase in  $v_{\text{corr}}$  above 2.5 mA/m<sup>2</sup>. Figure 4 shows, as an example, the chloride profiles measured when corrosion occurred on the upper (after 16 days) and middle (after 106 days) bars and after about 2 years of ponding on the specimen 15 %LI/0.61/300/CL2. The chloride profile was fitted with relationship (1) considering  $t$  equal to time of ponding

**Table 5** Chloride surface concentration,  $C_s$  (% vs binder), and diffusion coefficient,  $D_{app}$  ( $10^{-12}$  m<sup>2</sup>/s), after 2 years of exposure

Binder	$w/b$	Series curing (days)	CL1		CL2		CL3	
			7		7		28	
			$C_s$	$D_{app}$	$C_s$	$D_{app}$	$C_s$	$D_{app}$
		$b$ (kg/m <sup>3</sup> )						
OPC	0.61	300	–		4.51	6.5	–	
	0.46	300	1.83	4.21	1.62	3.03	1.95	5.6
	0.46	350	0.67	8.43	1.1	3.2	1.07	7.4
15 %LI	0.42	350	n.a.	n.a.	n.a.	n.a.	0.92	7.1
	0.61	250	–		2.6	15.2	–	
	0.61	300	–		6.14	16.4	–	
30 %LI	0.46	300	1.71	11.39	1.38	5.7	1.19	14.7
	0.46	350	2.76	4.30	1.31	7.78	1.28	5.5
	0.42	350	0.67	13.5	0.79	10.23	0.96	6.7
	0.42	400	1.33	4.7	2.31	4.83	0.96	3.9
30 %FA	0.61	300	–		3.4	27.8	–	
	0.46	300	1.43	14.5	2.84	18.2	2.42	13.56
	0.46	350	1.90	19.02	2.28	17.32	1.77	8.6
30 %PZ	0.42	350	1.96	2.52	1.35	8.2	1.54	7.6
	0.61	300	–		7.38	1.14	–	
	0.46	300	6.28	0.84	3.89	1.0	7.17	0.35
70 %BF	0.46	350	6.59	0.63	6.88	0.82	6.12	0.88
	0.42	350	3.29	0.42	3.89	0.43	5.33	0.47
	0.61	300	–		3.51	9.21	–	
30 %PZ	0.46	300	4.97	1.80	4.39	2.8	2.61	2.8
	0.46	350	3.01	2.4	2.05	1.9	2.35	2.9
	0.42	350	2.11	2.9	2.07	2.7	2.6	1.6
70 %BF	0.61	300	–		6.9	1.1	–	
	0.46	300	7.31	0.33	5.6	0.33	6.11	0.46
	0.46	350	5.13	0.36	7.92	0.20	6.80	0.24
	0.42	350	8.83	0.11	9.18	0.09	5.02	0.3

– = absence of specimen;  
n.a. = not available data

exposure and values of surface content  $C_s$  and apparent diffusion coefficient  $D_{app}$  were determined. Due to the high number of specimens, all the experimental profiles cannot be reported here and Table 4 summarises the results by showing the surface content  $C_s$  and the apparent diffusion coefficient  $D_{app}$  calculated by fitting each profile. Furthermore, Table 4 also shows the chloride content calculated from the profiles at the top ( $Cl_{top}$ ), average ( $Cl_{ave}$ ), and bottom ( $Cl_{bot}$ ) depth of the bar (for the upper bars depths of 10, 15 and 20 mm were considered respectively, for middle bars values depths of 25, 30 and 35 mm were taken into account and for lower bars, depths of 40, 45 and 50 mm were considered). In addition, after the end of the ponding phase chloride profiles were measured on all specimens and Table 5

summarises these results by showing the fitting values of  $C_s$  and  $D_{app}$  of the experimental profiles.

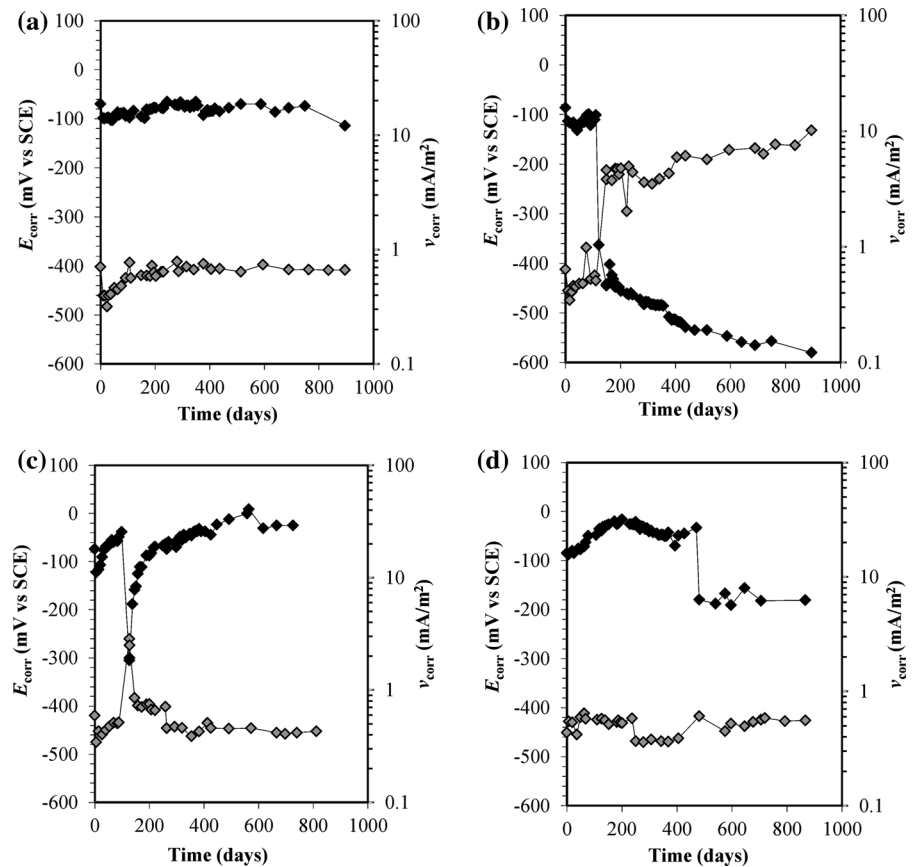
### 3.2 Ageing

After the interruption of the chloride ponding, specimens were kept in the dry atmosphere of the laboratory for approximately 1 year, then they were wetted with water for 1 month. The corrosion behaviour of all the rebars was measured before and during wetting. Figure 5 shows the relationship between the corrosion potential and the corrosion rate both in dry and wet conditions. The correlation between  $E_{corr}$  and  $v_{corr}$  was slightly different from the correlation obtained at the end of the ponding phase (Fig. 3). It can be observed that, in dry





**Fig. 2** Typical examples of corrosion potential ( $E_{\text{corr}}$ , black symbols) and corrosion rate ( $v_{\text{corr}}$ , grey symbols) trends as a function of time: middle bar (a) and upper bar (b) of specimen OPC/0.61/300/CL2, upper bar of specimen OPC/0.42/350/CL2 (c) and upper bar of specimen 15 %LI/0.46/300/CL3 (d)



condition, the corrosion potential values were in general higher than those at the end of the ponding phase (Fig. 3); this can be attributed to the rather dry condition of the concrete at the end of ageing. After wetting,  $E_{\text{corr}}$  of numerous rebars had rather low  $E_{\text{corr}}$ , lower than  $-250$  mV vs SCE. The bars that showed low  $E_{\text{corr}}$  values after wetting were more numerous than those that showed low  $E_{\text{corr}}$  values in the ponding phase. This suggests that some bars experienced corrosion initiation during the ageing. However, in most cases, even after 1 month of wetting  $v_{\text{corr}}$  was often still lower than  $1$  mA/m<sup>2</sup> on these bars. In order to investigate the possible onset of corrosion on these bars, potentiostatic tests were carried out.

### 3.3 Potentiostatic polarisation

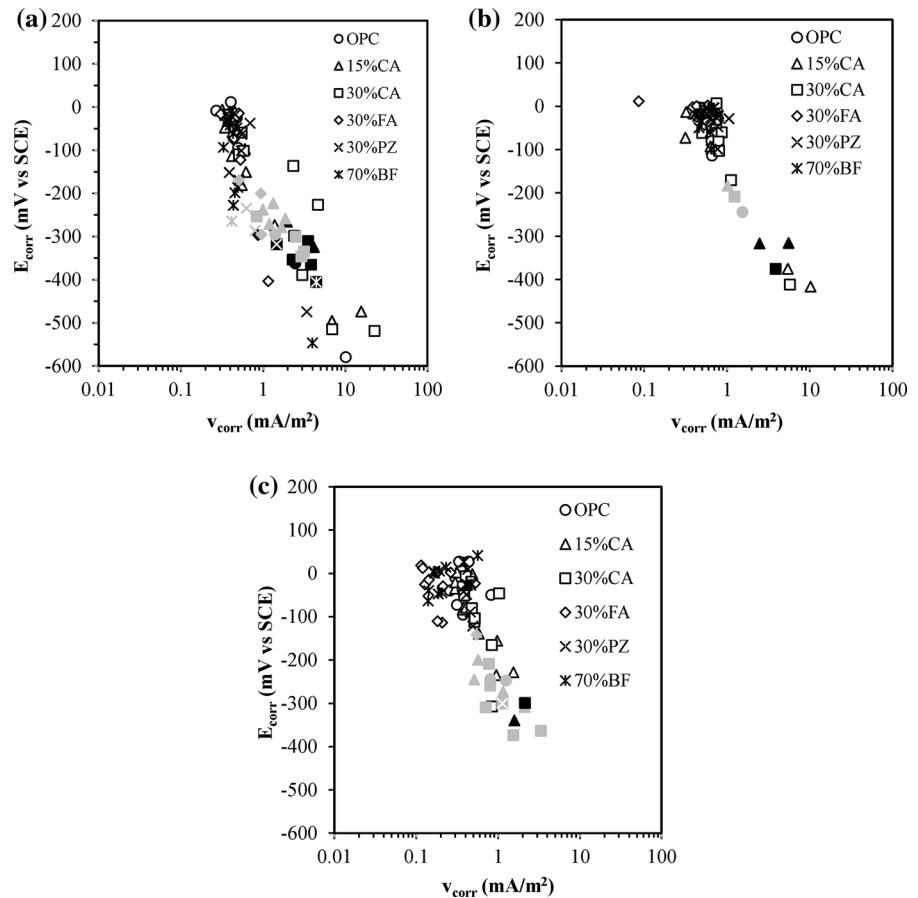
Potentiostatic anodic polarisation tests with steps of  $50$  mV were carried out on selected rebars. The correlation between the applied potential and

circulating current, measured after 1 h of polarisation, showed three different trends:

- the typical anodic behaviour of active steel, characterised by high values of current density even at low potential values (case a of Fig. 6);
- the typical behaviour of passive steel until the application of a potential of  $+600$  mV versus SCE, where the steel is brought to a condition of transpassivity ( $E_{\text{tr}}$ ) and the anodic reaction of oxygen evolution takes place on its surface (case b of Fig. 6);
- the typical behaviour of passive steel where the breakdown of the passive film occurs at a pitting potential  $E_{\text{pit}}$  (case c of Fig. 6).

Table 6 summarises the behaviour of the tested bars according to these three typical cases and shows the potential at which corrosion initiated ( $E_{\text{in}}$ ). 18 bars showed an active behaviour (a), showing that corrosion had already initiated before the potentiostatic test, i.e. in the ageing phase. Two of these bars (the upper

**Fig. 3** Relationship between the corrosion potential and corrosion rate of the three rebars—upper **a**, middle **b**, lower **c**—at the end of the ponding exposure (empty symbols), when corrosion initiated on active bars (black symbols) and in correspondence of the peaks of unstable periods (grey symbols)



bars of specimens 15 %LI/0.46/350/CL2 and 70 %BF/0.46/300/CL2) had shown, at the end of the ponding exposure, an undefined behaviour. For these bars the corrosion potential measured in dry condition, at the end of the ageing phase was taken into account as  $E_{in}$ . The other tested bars showed passive behaviours b and c. In 7 bars corrosion occurred during the polarisation tests (case c); in these specimens  $E_{in} = E_{pit}$  and values between  $-250$  and  $+300$  mV versus SCE were determined. In the remaining cases, bars were passive up to  $E_{tr}$ , so  $E_{in} > 600$  mV versus SCE.

### 3.4 Final observations

At the end of the tests, bars were extracted from the concrete for visual observation, and the chloride content was measured on the concrete samples ground near the top and bottom steel surface,  $Cl_{grind}$  as shown in Fig. 1. Results of visual observation and chloride

content obtained on bars that experienced corrosion initiation during the ponding phase are shown in Table 4. In particular it was evaluated if the bars showed attacks of limited extent (low level of corrosion) or an extended corroded surface which interested the whole surface or a broad portion of the surface (high level of corrosion). Most of these bars showed an extended corroded surface.

Results of visual observation and chloride content of bars subjected to potentiostatic tests are summarized in Table 6. Penetrating attacks of limited extent were observed on bars where the breakdown of the protective film occurred during or before the polarisation test (cases a and c of Fig. 6). As expected, no signs of corrosion were visible on bars with the passive behaviour b.

Careful observation of the initiation sites showed that corrosion did not only initiate on the top of the bars (i.e. where higher chloride content is expected). As a matter of fact, some bars showed corrosion only

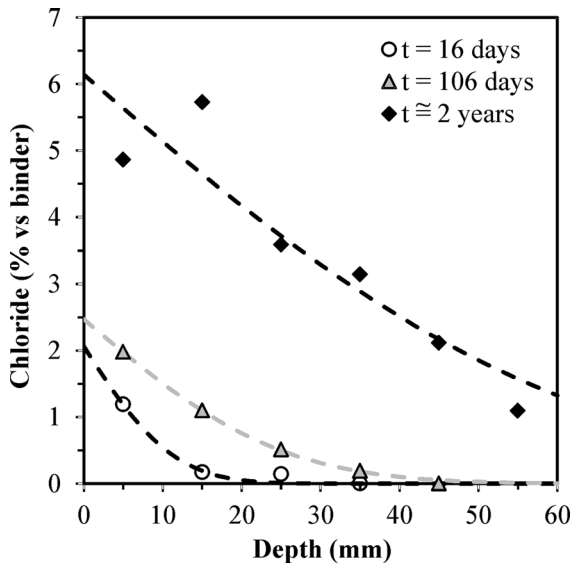


**Fig. 4** Example of chloride profiles measured on concrete core taken in non-reinforced part of the specimen 15 %LI/0.61/300/CL2 (white symbols chloride measured when corrosion initiated on the upper bar; grey symbols chloride measured when corrosion occurred on the middle bar; black symbols chloride measured at the end of ponding exposure)

in the top side, whilst other bars only in the bottom side (where chloride content is lower, but effects of bleeding on concrete microstructure are expected to be more relevant). Even mixed conditions occurred. For instance, the middle bar of the specimen 15 %LI/0.61/250/CL2 showed the presence of pits in the bottom side, whilst in the lower bar embedded in the same specimen corrosion occurred in the top side.

Furthermore, no effect of compaction voids present at the steel–concrete interface could be observed. Although macropores with diameter up to several millimetres were present at the concrete/steel interface, they did not act as preferential sites for corrosion initiation.

## 4 Discussion

It is well known that supplementary cementing materials (SCMs) with pozzolanic or hydraulic properties have a key role in defining the resistance of concrete to the penetration of chloride ions [11, 13, 14, 18, 36, 37, 42, 51]. The beneficial role of natural pozzolan (PZ), coal fly ash (FA) and blast-furnace slag (BF) was confirmed also in this work, as shown by the

lowering in the apparent chloride diffusion coefficients induced by these additions compared to concrete with portland cement or addition of ground limestone (Table 5). Nevertheless, the positive influence of SCMs on the service life of RC structures exposed to chloride environment may be mitigated if they had a negative influence on the chloride threshold of steel corrosion initiation, as suggested by several Authors [41, 49, 53]. This work started with the optimistic aim of determining the chloride threshold for steel reinforcing bars embedded in concrete with a wide range of SCMs under constant exposure conditions. Following the suggestion of many Authors [8, 32, 46], in order to reproduce more ‘realistic’ conditions, long-term tests were planned with penetration of chloride ions through ponding and rebars were left in free corrosion conditions (without any external perturbation, apart from negligible polarisation during polarisation resistance measurements). Nevertheless, during more than 2 years of the ponding phase plus 1 year of ageing phase a series of limitations of this approach emerged both for the detection of corrosion initiation and the measurement of the chloride content. These will be discussed first and, then, the results of the tests will be analysed in relation to the influence of SCMs.

### 4.1 Measurement of the chloride threshold

The chloride threshold  $Cl_{th}$  may be defined as:

$$Cl_{th} = Cl(x, t_{in})$$

where  $Cl(x, t_{in})$  is the amount of chlorides in the concrete measured at the depth of the bar ( $x$ ) and at the time when corrosion initiates ( $t_{in}$ ). Hence, to evaluate the critical chloride threshold, there are two critical steps: the detection of the initiation time ( $t_{in}$ ) followed by the (immediate) measurement of the chloride content near the steel surface.

#### 4.1.1 Detection of the onset of corrosion

When reinforcing bars are left in free corrosion conditions, corrosion initiation due to chloride penetration may be detected by corrosion potential and corrosion rate measurements, as shown in Fig. 2b. In this work, in agreement with other Authors [2, 6, 25], a criterion based on a potential decrease below  $-250$  mV versus SCE or a corrosion rate increase

**Fig. 5** Relationship between the corrosion potential and corrosion rate of the three rebars—upper **a**, middle **b**, lower **c**—at the end of the ageing period (empty symbols) and in wet condition (grey symbols) (OPC concretes are not shown)

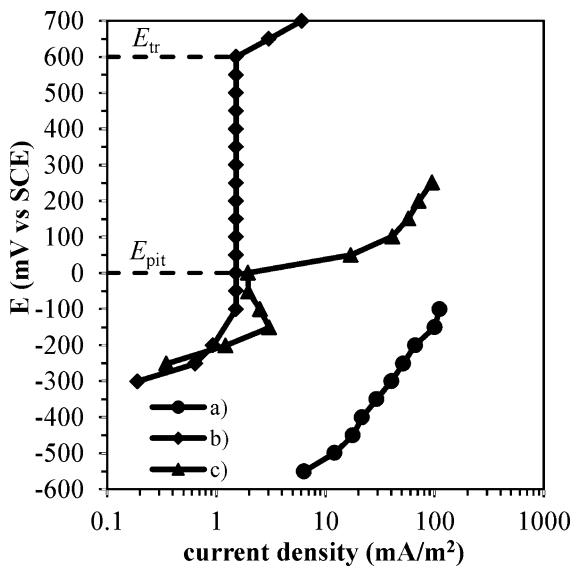
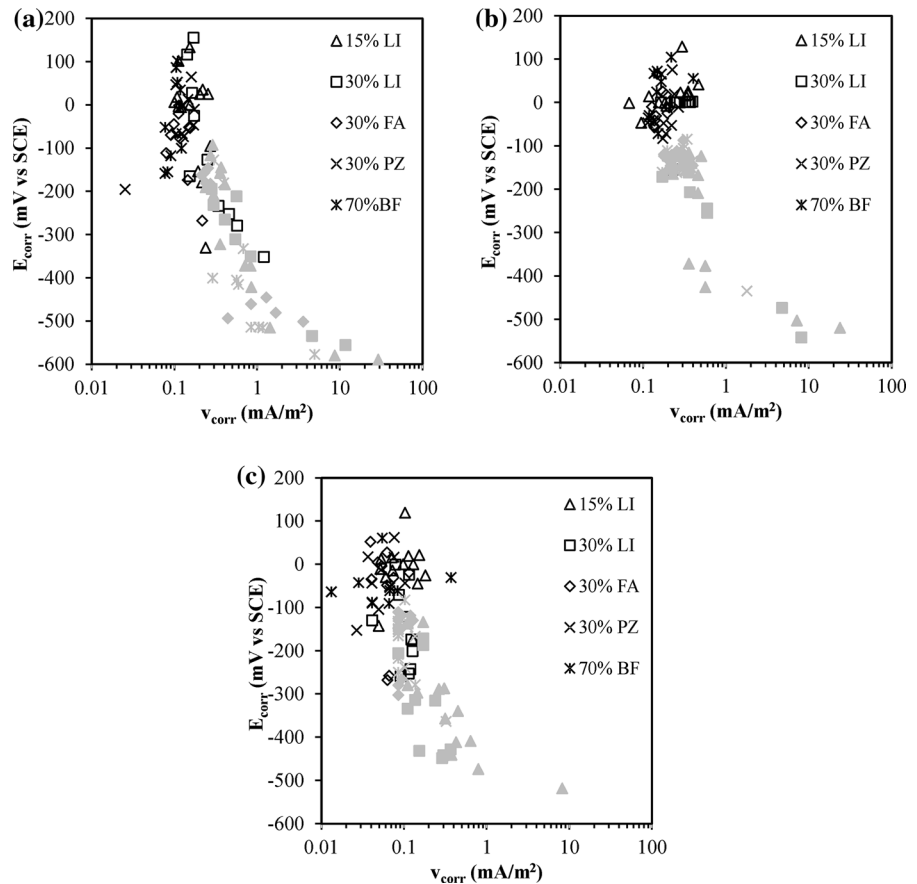


**Fig. 6** Typical examples of polarisation curves: active steel (a), passive steel, with indication of  $E_{tr}$  (b) and steel where corrosion initiated during the polarisation step above  $E_{pit}$  (c)

above  $2.5 \text{ mA/m}^2$  was assumed a priori in order to detect the time when the chloride measurement was necessary. However, the example of Fig. 2c shows that unstable conditions may occur where the chloride amount at the bars depth is sufficient to nucleate a pit but it is unable to sustain its growth, and repassivation occurs. Since usually the initiation of corrosion is associated with the development of pits able to propagate spontaneously [5], a continuous monitoring in time of the corrosion parameters is necessary even after the abrupt change is detected. Although monitoring for 1 week after the potential drop has been proposed by some Authors to confirm the bar active state [24], the results of this work show that a longer period could be necessary. Passive/active transition, which takes place over a period of time rather than being a one-step occurrence [8, 16], occurred usually within about 2 weeks; however for some specimens a more prolonged time was needed to significantly break the passivity film. Detection of corrosion initiation is

**Table 6** Bars behaviour detected during the polarisation tests (in accordance with the three cases depicted in Fig. 6), potential when corrosion initiated,  $E_{in}$ , chloride content measured with grinding near the bar sites,  $Cl_{grind}$ , and results of visual observation, V.O.

Binder	$w/b$	$b$ (kg/m <sup>3</sup> )	Series	Bar	Bar behaviour (Fig. 6)	$E_{in}$ (mV vs SCE)	$Cl_{grind}$ (% vs binder)		V.O.	
							Top	Bottom	Top	Bottom
15 %LI	0.46	300	CL1	u	<i>c</i>	−150	1.38	1.19	–	✓✓
				l	<i>a</i>	−30	1.12	0.21	✓✓	✓✓
15 %LI	0.46	300	CL2	u	<i>c</i>	0	1.24	0.93	✓✓	✓✓
				m	<i>a</i>	+14	0.38	0.30	✓✓	✓
				l	<i>a</i>	+12	0.36	0.53	✓✓	✓
15 %LI	0.46	300	CL3	u	<i>c</i>	+100	1.45	1.51	✓	✓
				m	<i>a</i>	−47	1.45	1.93	–	✓✓
				l	<i>a</i>	−45	2.02	1.65	✓	✓✓
15 %LI	0.46	350	CL1	u	<i>a</i>	+18	1.75	2.23	–	✓✓
				m	<i>b</i>	>+600	1.39	0.42	–	–
15 %LI	0.46	350	CL2	u	<i>a</i>	0	1.86	1.84	–	✓✓
				m	<i>b</i>	>+600	0.84	0.17	–	–
15 %LI	0.42	350	CL1	u	<i>c</i>	+302	0.89	0.66	✓	–
				m	<i>b</i>	>+600	0.45	0.24	–	–
				l	<i>b</i>	>+600	0.23	0.37	–	–
15 %LI	0.42	350	CL2	u	<i>b</i>	>+600	0.72	0.18	–	–
				m	<i>b</i>	>+600	0.24	0.18	–	–
				l	<i>b</i>	>+600	0.19	0.18	–	–
30 %LI	0.46	300	CL1	u	<i>c</i>	−252	2.04	2.44	✓✓	✓✓
				m	<i>c</i>	0	1.69	1.19	✓✓	✓✓
				l	<i>a</i>	−253	1.17	0.77	–	✓✓
30 %LI	0.46	300	CL3	m	<i>c</i>	−50	1.79	1.22	✓✓	–
30 %FA	0.46	300	CL1	u	<i>a</i>	−112	5.84	0.47	✓✓	–
				m	<i>b</i>	>+600	0.33	0.3	–	–
30 %FA	0.46	300	CL2	u	<i>a</i>	−45	3.80	0.83	✓✓	–
				m	<i>b</i>	>+600	0.32	0.37	–	–
				l	<i>b</i>	>+600	0.43	0.32	–	–
30 %FA	0.46	300	CL3	u	<i>a</i>	−21	2.34	0.84	✓✓	–
				m	<i>b</i>	>+600	0.15	0.39	–	–
				l	<i>b</i>	>+600	0.15	0.48	–	–
30 %PZ	0.46	300	CL1	m	<i>b</i>	>+600	0.99	0.43	–	–
				l	<i>a</i>	−13	0.10	0.52	–	✓✓
30 %PZ	0.46	300	CL2	u	<i>a</i>	+46	2.75	2.18	✓✓	✓✓
				m	<i>b</i>	>+600	0.73	0.71	–	–
				l	<i>a</i>	+17	0.33	0.12	–	✓✓
30 %PZ	0.46	300	CL3	u	<i>a</i>	+64	2.72	2.21	✓✓	✓✓
				m	<i>b</i>	>+600	0.63	0.51	–	–
70 %BF	0.46	300	CL1	m	<i>b</i>	>+600	0.40	0.27	–	–
70 %BF	0.46	300	CL2	u	<i>a</i>	−159	2.78	0.50	✓✓	–
				m	<i>b</i>	>+600	0.42	0.21	–	–
				l	<i>a</i>	−61	3.34	1.35	–	✓✓
70 %BF	0.46	300	CL3	u	<i>a</i>	−7	0.40	0.29	✓✓	–
				m	<i>b</i>	>+600	0.37	0.45	–	–

– = no sign of corrosion; ✓✓ = low level of corrosion, i.e. in a limited area; ✓✓ = high level of corrosion, i.e. present on the whole surface of the bars or a broad portion of the surface



further complicated by the presence of undefined cases as those shown in Fig. 2d.

Table 3 shows that corrosion initiated only on 15 bars, whilst for the rest of the 192 bars tested in this work no corrosion onset could be detected after two and a half years of ponding (case of Fig. 2a), even on bars that had a concrete cover of only 10 mm. Specifically, no corrosion initiation was detected on rebars in concrete with high resistance to chloride penetration (i.e. concrete with low water/binder ratio and the use of fly ash and blast furnace slag). On the one hand this shows that ponding tests may not provide useful results for the evaluation of the chloride tests even after long times, especially for those concrete compositions of more interest for chloride-bearing environments. On the other hand, it raises the question whether exposure under free-corrosion conditions of specimens subjected to ponding is really representative of real structures. In fact, several rebars showed corrosion initiations during the ageing phase, when the specimens were left to dry for about 1 year (thus allowing their corrosion potential to raise to higher values, where corrosion initiation is favoured [43]). By wetting the specimens at the end of the ageing period, these bars, in fact, showed a decrease in  $E_{\text{corr}}$  compared to the values previously measured during the ponding phase. Initiation of corrosion of these bars, however, could only be clearly detected by means of potentiostatic polarisation tests, when cases a and c of Fig. 6 were observed. Table 6 shows that corrosion could be detected on further 25 bars. Potentiostatic polarisation, although it induces some perturbation to the steel, appeared to be more discriminant in the detection of corrosion onset than the monitoring of  $E_{\text{corr}}$  and  $v_{\text{corr}}$ . Furthermore, the stepwise polarisation procedure followed in this work allowed determining the potential at which corrosion initiated ( $E_{\text{in}}$ , Table 6), which is an important parameter affecting corrosion initiation [43, 3, 12]. These results suggest that ponding tests on specimens with bars under free-corrosion conditions may not be really representative of exposure conditions of real structures, since they bring about values of  $E_{\text{corr}}$  rather stable, due to the constant exposure of the bars to moist concrete, and they do not reproduce the typical fluctuation in potential of bars due to changes in time of the concrete moisture content (e.g. due to splashes or raining followed by drying). As a matter of fact in atmospheric conditions potential values between

–200 mV vs SCE and +200 mV vs SCE can be measured, whilst in the tidal zone values between -500 mV and +100 mV vs SCE can be obtained [23, 33, 44].

#### 4.1.2 Evaluation of the chloride content

Two approaches can be used for the measurement of the chloride content in specimens aimed at the determination of the chloride threshold: the sampling of concrete near the steel surface (in some case even near the corrosion spot [3]) or the measurements in remote sites at the same depth of the bars. Although the first method might appear more appropriate since it gives a localised information, it requires the demolition of the specimens as soon as corrosion is detected. Therefore, errors in the early interpretation of the onset of corrosion from  $E_{\text{corr}}$  and  $v_{\text{corr}}$  measurements may lead to wrong estimation of the chloride threshold (e.g. if repassivation takes place). The sampling of concrete far from the bar has the advantage that the removal of the bar is not required and the exposure continues allowing a clearer detection of corrosion initiation.

In this work both methods of sampling were performed. Cores in the non-reinforced part of the specimens were taken each time corrosion was detected (and only from further monitoring of the bars it could be verified if corrosion initiation was stable) and at the end of the ponding phase. Chloride profiles were then measured (Tables 4, 5) and, by fitting with Eq. (1), the value at the top, middle and bottom of bars were calculated. Sampling of the chloride content near the steel bars was carried out by manual grinding within a depth of 1–2 mm at the top and the bottom of each bar site when the specimens were splitted at the end of the tests (Table 6).

Figure 7 compares the chloride contents measured on the concrete cores taken after the interruption of the ponding and the content measured on the concrete samples ground from the bar sites after the breaking of the specimens (no more chlorides had penetrated after the interruption of the ponding). For both techniques, values at the top and bottom of each bar are shown. A significant scatter of results can be observed. This is common for this type of measurements, especially for the manual grinding of small samples near the steel surface (where the ratio between cement paste and aggregates may be quite variable). Nevertheless, some



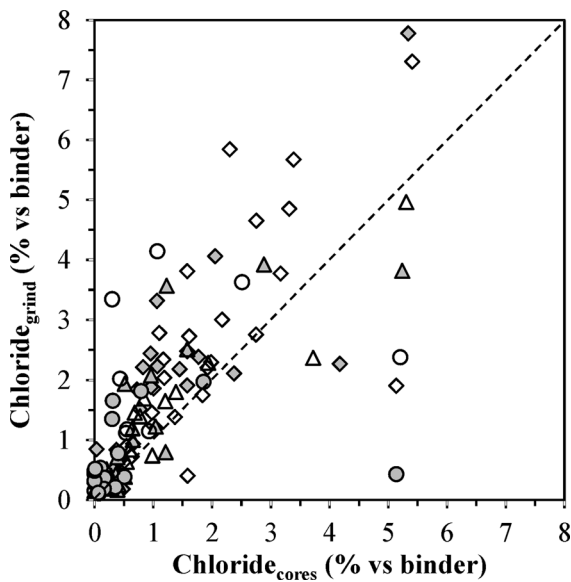


**Fig. 7** Comparison between the chloride content evaluated from chloride profile measured at the end of the ponding phase ( $Cl_{cores}$ ) and from concrete powders collected from the bar sites after ageing ( $Cl_{grind}$ ). Symbols distinguish between *upper* (diamonds), *middle* (triangles) and *lower* (circles) bars. White symbols top of bar; grey symbols bottom of bar

relationships between the results of the two methods were found. In general, the chloride content measured by the concrete cores was slightly lower than the chloride content at the bar sites, which can be explained by the different location of the sampling: according to [57] and [48], the amount of chlorides around the top of the rebar could be higher than that at the same depth away from the rebar owing to the relatively low content of coarse aggregates in the vicinity of the rebar and to a physical barrier effect of the bar itself. Furthermore, since grinding was carried out about 1 year after coring, it cannot be excluded that some redistribution of chloride could have occurred during the ageing phase (although concrete was rather dry).

In our opinion results from cores, being obtained from the interpolation of bulk concrete samples taken at different depths, might be considered a more reliable estimation of the chloride content at the depth of the bars. Thus values extrapolated from chloride profiles will be considered in the following section.

Nevertheless, a further problem in the detection of the chloride content is the reference depth. Visual observation of the bars at the end of the tests (Tables 4,

6) showed that corrosion did not always initiate at the top side of the bars (where the chloride content was higher), in accordance to similar observations reported by other Authors [8]. Table 4 shows that the difference between the chloride contents measured at top ( $Cl_{top}$ ) and bottom ( $Cl_{bot}$ ) depths of bars where corrosion initiated can be up to 0.6 % by mass of binder or even higher for the concrete made with fly ash (due to the high chloride surface concentration and the low diffusion coefficient). This large variation makes the definition of the chloride threshold difficult. Considering  $Cl_{bot}$  would be on the safe side, leading to an underestimation of the service life and for example the adoption of more restrictive prescriptions on the concrete composition. Conversely, considering  $Cl_{up}$  could lead to an overestimation of the service life and to a premature failure of the structure.

Therefore, the results of this work show that the measure of the chloride threshold on specimens subjected to chloride penetration, besides being quite time-consuming, is affected by a series of criticalities related to both the detection of corrosion initiation and the evaluation of the ‘appropriate’ chloride content.

#### 4.2 Effect of SCMs

In spite of the limitations described in the previous section, an attempt can be made to estimate the chloride threshold for the concrete compositions studied in this work and assess the role of the supplementary cementing materials.

Firstly, the bars where corrosion initiation was detected during the ponding phase (Table 4) or during ageing or potentiostatic tests (Table 6) can be considered. Figure 8 shows the chloride content estimated from chloride profiles at the depth of these bars (the symbols show the value at the centre of the bar,  $Cl_{ave}$ , while the scatter band shows the range between  $Cl_{bot}$  and  $Cl_{top}$ ). Since the potential affects the critical chloride threshold, only results of potentiostatic polarisation tests where  $E_{in}$  was in the range of +100/−100 mV vs SCE were taken into account. Ranges shown in Fig. 8 may be assumed as an estimation of the chloride threshold for these bars. Empty square symbols also show the chloride content measured at the location where corrosion initiation was detected by visual observation of the bars, i.e. on top side or bottom side respectively if corrosion was

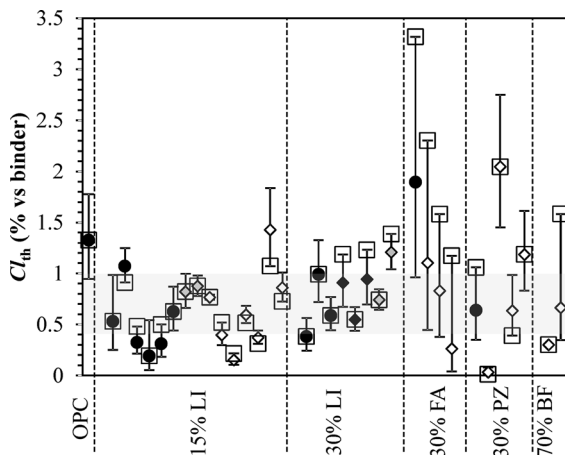


**Fig. 8** Chloride contents estimated from chloride profiles (*top*, average and *bottom* depths) on the bars when corrosion initiated during ponding (*black*), ageing (*white*) or polarisation tests (*grey*). Symbols show the water/binder ratio of concrete (*circle* = 0.61, *diamond* = 0.46, *triangle* = 0.42). The *squares* show the position where corrosion initiation was detected from visual observation. *Grey* area indicates the range 0.4–1 % by mass of cement

observed only or mainly on one of these sides or the average depth in the other cases.

To have an indication of the lower bound of the critical chloride threshold also from some of the large number of bars that did not show corrosion initiation during the tests, Fig. 9 shows the chloride content

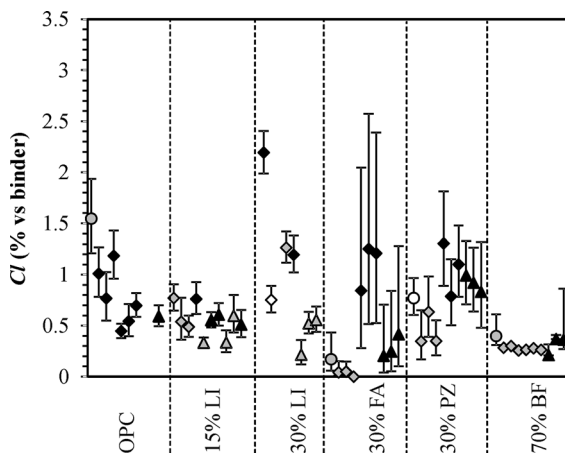


**Fig. 9** Chloride contents estimated from chloride profiles (*top*, average and *bottom* depths) on the passive bars at the end of the ponding phase. Symbols show the water/binder ratio of concrete (*circle* = 0.61, *diamond* = 0.46, *triangle* = 0.42). Colours define the position of the bar *upper* (*black*), *middle* (*grey*) *lower* (*white*)

measured on the outermost bars where corrosion did not initiate neither during ponding nor the potentiostatic tests.

In spite of the relatively small number of available data, some considerations on the role of the type of cement can be made, whilst the large variability of results and the limited number of useful results do not allow an evaluation of the effect of the water/binder ratio and cement content.

Figure 8 shows that bars in concrete with addition of ground limestone (15 %LI and 30 %LI) had chloride threshold values,  $Cl_{ave}$ , in the range between 0.15 and 1.4 % by mass of binder, with a mean value of 0.7 % by mass of binder evaluated by considering all data. The majority of results fall in the typical range of 0.4–1 % by mass of binder reported in the literature for RC structures exposed to the atmosphere, although several values below or above this range can be observed (as for instance for the specimen with 15 % limestone and  $w/b = 0.61$  where on the upper bar a  $Cl_{ave}$  of 0.19 % by mass of binder was measured). Also the chloride content where corrosion initiation was detected by visual observation of the bars (square symbols in Fig. 8) was within this range. The chloride contents reported in Fig. 9 show that, even on the bars that remained passive, chloride contents at the end of the tests were comparable to those measured in the bars where corrosion initiation took place; chloride contents higher than 1 % by mass of binder were measured in several cases. This confirms the random nature of pitting corrosion initiation and supports the search for a statistical approach for its evaluation, which is, however, inapplicable in practice with ponding tests considering the previously described difficulties in obtaining valid experimental results.

Unfortunately only one chloride value, equal to 1.3 % by mass of binder, could be associated to corrosion initiation for bars embedded in portland cement concrete (OPC) and, hence, the chloride threshold in this type of binder cannot be derived from the results of this work. Some effect of the pozzolanic and hydraulic additions may, conversely, be inferred from Fig. 8, where higher values of the chloride threshold can be observed for PZ and FA concrete. In concretes with natural pozzolan cement, a mean value of 0.9 % by mass of binder was measured ( $Cl_{ave}$  was 0.1–2 % by mass of cement). In fly ash concrete,  $Cl_{ave}$  was between 0.3 and 1.9 % by mass of binder, with a mean value of 1 % by mass of binder.



However, chloride content values measured where corrosion initiated (square symbols) support the hypothesis that the critical chloride content is even higher for fly ash concrete. Also chloride contents measured on passive bars embedded in fly ash and pozzolanic concretes were higher than those that promoted corrosion in limestone concrete (Fig. 9). The number of useful results in concrete with pozzolanic additions is, however, quite limited due to its high resistance to chloride penetration. Only two chloride values leading to corrosion initiation are available for BF concrete, and they are quite different. Therefore for BF concrete it is not possible to derive any useful information about the chloride threshold. It should also be observed that the chloride content of 0.18 % by mass of binder introduced by the slag may have affected the initial passivation of the steel, negatively affecting its resistance against depassivation due to subsequent chloride penetration.

Due to the lack of clear critical chloride threshold, no statistical treatment could be made on OPC and BF concretes, whilst regarding the LI, PZ and FA mixes, Fig. 10 shows the relative cumulative frequency of the critical chloride threshold obtained considering the chloride content measured at the location where corrosion initiation was detected by visual observation of the bars (square symbols in Fig. 8). It can be observed that the relative cumulative frequency of the

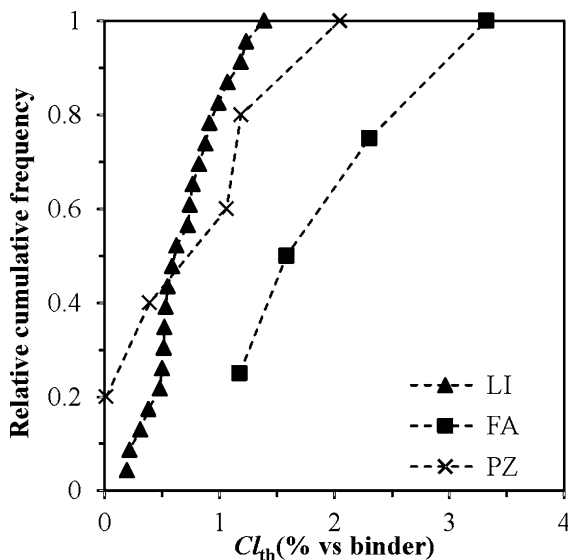


**Fig. 10** Relative cumulative frequency of the critical chloride threshold for limestone, natural pozzolan and fly ash concretes

critical chloride threshold for FA concretes was shifted to the right compared to LI concretes, suggesting, as previously observed, a higher value of the chloride threshold for fly ash in comparison to limestone concretes. The relative cumulative frequency of critical chloride threshold for natural pozzolan concretes showed a higher scatter compared to those of limestone and fly ash concretes, with an upper limit in between the values of limestone and fly ash. In order to refine the evaluation of the relative cumulative frequency, further research is needed and, in the opinion of the Authors, new test procedures should be developed that are able to provide a number of results sufficient for statistical evaluations in a reasonable time.

## 5 Conclusions

Ponding tests on concrete specimens with bars in free corrosion conditions showed to be unsuitable for the study of the chloride threshold of steel in concrete. After two and half years of ponding, corrosion initiation could be detected only on a rather limited number of bars (15 out of a total number of 192). Even on the outmost bars, with a concrete cover of only 10 mm, corrosion occurred on few specimens (9 out of 64, i.e. <15 %). Although this type of test is often suggested because it is a priori assumed to be more representative of real exposure conditions, its long duration made it unsuitable for the measurement of the critical chloride threshold, especially for concrete with high resistance to chloride penetration. Furthermore, the ageing phase showed that the moist condition of concrete induced by ponding may prevent corrosion that can conversely initiate under drier conditions.

Even when corrosion initiation could be detected, the measurement of the chloride content was a second critical step. Both the sampling procedure (i.e. local grinding near the bar or remote determination of chloride profiles), and the location on the bars (i.e. top position, where chloride content was higher, or the exact position where corrosion initiation was detected), had a remarkable influence on the measured chloride content and thus on the estimated value of the chloride threshold.

Despite the experimental problems and the consequent limited number of useful data, results of this work suggested higher critical chloride threshold

values for concrete with natural pozzolan or fly ash cements compared to concrete with portland-lime-stone cements.

**Acknowledgements** This research was financed by the Italian Ministry of University and Research (MIUR), Holcim Italia S.p.A. and Sismic.

## References

- Alonso C, González JA (1978) Quantitative measurements of corrosion rate of reinforcing steels embedded in concrete using polarization resistance measurements. *Mater Corr* 29(8):515–519. doi:10.1002/maco.19780290804
- Alonso C, Andrade C, Castellote M, Castro P (2000) Chloride threshold values to depassivate reinforcing bars embedded in a standardised OPC mortar. *Cement Concrete Res* 30(7):1047–1055. doi:10.1016/S0008-8846(00)00265-9
- Alonso C, Castellote M, Andrade C (2002) Chloride threshold dependence of pitting potential of reinforcements. *Electrochim Acta* 47(21):3469–3481. doi:10.1016/S0013-4686(02)00283-9
- Alonso MC, Sanchez M (2009) Analysis of the variability of chloride threshold values in the literature. *Mater Corros* 60(8):631–637. doi:10.1002/maco.200905296
- Andrade C (2003) Determination of the chloride threshold in concrete. In: Cigna R, Andrade C, Nürnberger U, Polder R, Weydert R, Seitz E (eds), *Corrosion of steel in reinforced concrete structures*, Luxembourg: COST 521, Final Report, pp 101–111
- Andrade C, Alonso C, Gulikers J, Polder RB, Cigna R, Vennesland Ø, Salta M (2004) RILEM TC-154-EMC: electrochemical techniques for measuring metallic corrosion. Test methods for on-site corrosion rate measurement of steel reinforcement in concrete by means of the polarization resistance method. *Mater Struct* 37:623–643
- Angst U, Elsener B, Larsen CK, Vennesland Ø (2009) Critical chloride content in concrete: a review. *Cement Concrete Res* 39(12):1122–1138. doi:10.1016/j.cemconres.2009.08.006
- Angst UM, Elsener B, Larsen CK, Vennesland O (2011) Chloride induced reinforcement corrosion: electrochemical monitoring of initiation stage and chloride threshold values. *Corros Sci* 53(4):1451–1464. doi:10.1016/j.corsci.2011.01.025
- Ann KY, Song H-W (2007) Chloride threshold level for corrosion of steel in concrete. *Corros Sci* 49(11):4113–4133. doi:10.1016/j.corsci.2007.05.007
- Bertolini L (2008) Steel corrosion and service life of reinforced concrete structures. *Struct Infrastruct Eng* 4(2):123–137. doi:10.1080/15732470601155490
- Bertolini L, Lollini F, Redaelli E (2008) Concrete composition and service life of reinforced concrete structures exposed to chloride bearing environments. In: Biondini F, Frangopol M (eds) *Life-cycle civil engineering*. CRC Press, London, pp 113–118
- Bertolini L, Bolzoni F, Gastaldi M, Pastore T, Pedferri P, Redaelli E (2009) Effects of cathodic prevention on the chloride threshold for steel corrosion in concrete. *Electrochim Acta* 54(5):1452–1463. doi:10.1016/0950-0618(95)00017-8
- Bertolini L, Carsana M, Frassoni M, Gelli M (2011) Pozzolanic additions for durability of concrete structures. *Proc ICE-Constr Mater* 164(6):283–291. doi:10.1680/coma.1000041
- Bertolini L, Lollini F, Redaelli E (2011) Comparison of resistance to chloride penetration of different types of concrete through migration and ponding tests. In: Andrade C, Mancini G (eds) *Modelling of corroding concrete structures*, vol 5. RILEM Bookseries, Bookseries, pp 125–135
- Bertolini L, Elsener B, Pedferri P, Redaelli E, Polder R (2013) *Corrosion of steel in concrete: prevention, diagnosis, repair*, 2nd edn. Wiley VCH, Weinheim
- Bouteiller V, Cremona C, Baroghel-Bouny V, Maloula A (2012) Corrosion initiation of reinforced concretes based on Portland or GGBS cements: chloride contents and electrochemical characterizations versus time. *Cement Concrete Res* 42:1456–1467. doi:10.1016/j.cemconres.2012.07.004
- Breit W, Schiessl P (1997) Investigation on the threshold value of the critical chloride content. In: *Fourth CANMET/ACI Conference on durability of concrete*. ACI SP70, Detroit, vol 2, pp 363–372
- Carsana M, Frassoni M, Bertolini L (2014) Comparison of ground-waste-glass with other supplementary cementitious materials. *Cem Concr Compos* 45:39–45. doi:10.1016/j.cemconcomp.2013.09.005
- Castellote M, Andrade C, Alonso C (2002) Accelerated simultaneous determination of the chloride depassivation threshold and of the non-stationary diffusion coefficient values. *Corros Sci* 44(11):2409–2424. doi:10.1016/S0010-938X(02)00060-4
- Cheewaket T, Jaturapitakkul C, Chalee W (2012) Initial corrosion presented by chloride threshold penetration of concrete up to 10 year-results under marine site. *Constr Build Mater* 37:693–698. doi:10.1016/j.conbuildmat.2012.07.061
- Choi Y-S, Kim J-G, Lee K-M (2006) Corrosion behavior of steel bar embedded in fly ash concrete. *Corros Sci* 48(7):1733–1745. doi:10.1016/j.corsci.2005.05.019
- Frederiksen JM (2009) On the need for more precise threshold values for chloride initiated corrosion. *Mater Corros* 60(8):597–601. doi:10.1002/maco.200905273
- Frølund T, Klinghoffer O, Sørensen HE (2003) Pro's and con's of half-cell potentials and corrosion rate measurements. In: *International Conference on "Structural faults + repairs"*, London
- Garcia V, Francois R, Carcasses M, Gegout P (2014) Potential measurement to determine the chloride threshold concentration that initiates corrosion of reinforcing steel bar in slag concrete. *Mater Struct* 47:1483–1499. doi:10.1617/s11527-013-0130-5
- Geng C, Xu Y, Weng D, Wu X (2010) A time-saving method to determine the chloride threshold level for depassivation of steel in concrete. *Constr Build Mater* 24(6):903–909. doi:10.1016/j.conbuildmat.2009.12.002
- Glass GK, Page CL, Short NR (1991) Factors affecting the corrosion rate of steel in carbonated mortars. *Corros Sci* 32(12):1283–1294



27. Glass GK, Buenfeld NR (1997) The presentation of the chloride threshold level for corrosion of steel in concrete. *Corros Sci* 39(5):1001–1013. doi:[10.1016/S0010-938X\(97\)00009-7](https://doi.org/10.1016/S0010-938X(97)00009-7)
28. Hartt WH, Nam J (2008) Effect of cement alkalinity on chloride threshold and time-to-corrosion of reinforcing steel in concrete. *Corrosion* 64(8):671–680. doi:[10.5006/1.3279929](https://doi.org/10.5006/1.3279929)
29. Hussain SH, Rasheeduzzafar (1994) Corrosion resistance performance of fly ash blended cement concrete. *ACI Mater J* 91(3):264–272. doi:[10.14359/4332](https://doi.org/10.14359/4332)
30. Hussain SE, Rasheeduzzafar Al-Musallam A, Al-Gahtani AS (1995) Factors affecting threshold chloride for reinforcement corrosion in concrete. *Cement Concrete Res* 25(7):1543–1555. doi:[10.1016/0008-8846\(95\)00148-6](https://doi.org/10.1016/0008-8846(95)00148-6)
31. Hussain SH, Al-Gahtani AS, Rasheeduzzafar (1996) Chloride threshold for corrosion of reinforcement in concrete. *ACI Mater J* 93(6):534–538. doi:[10.14359/9857](https://doi.org/10.14359/9857)
32. Lambert P, Page CL, Vassie PRV (1991) Investigations of reinforcement corrosion. 2. Electrochemical monitoring of steel in chloride-contaminated concrete. *Mater Struct* 24:351–358
33. Lau K, Sagues AA, Yao L (2005) Corrosion performance of concrete cylinder piles. Final Report to Florida Department of Transportation, Tampa
34. Lollini F, Redaelli E, Bertolini L (2014) Effects of portland cement replacement with limestone on the properties of hardened concrete. *Cement Concrete Comp* 46:32–40. doi:[10.1016/j.cemconcomp.2013.10.016](https://doi.org/10.1016/j.cemconcomp.2013.10.016)
35. Manera M, Vennesland Ø, Bertolini L (2008) Chloride threshold for rebar corrosion in concrete with addition of silica fume. *Corros Sci* 50(2):554–560. doi:[10.1016/j.corsci.2007.07.007](https://doi.org/10.1016/j.corsci.2007.07.007)
36. Massazza F (1998) Pozzolana and Pozzolanic cements. In: Hewlett PC (ed) *Lea's chemistry of cement and concrete*, 4th edn. Arnold Publishers, London
37. Mehta PK, Monteiro PJM (2006) *Concrete: microstructure, properties and materials*. McGraw-Hill, New York
38. Mohammed TU, Hamada H (2006) Corrosion of steel bars in concrete with various steel surface conditions. *ACI Mater J* 103(4):303–311. doi:[10.14359/16606](https://doi.org/10.14359/16606)
39. Morris W, Vico A, Vazquez M, De Sanchez SR (2002) Corrosion of reinforcing steel evaluated by means of concrete resistivity measurements. *Corros Sci* 44(1):81–99. doi:[10.1016/S0010-938X\(01\)00033-6](https://doi.org/10.1016/S0010-938X(01)00033-6)
40. Nygaard PV, Geiker MR (2005) A method for measuring the chloride threshold level required to initiate reinforcement corrosion in concrete. *Mater Struct* 38(4):489–494. doi:[10.1617/14279](https://doi.org/10.1617/14279)
41. Oh BH, Jang SY, Shin YS (2003) Experimental investigation of the threshold chloride concentration for corrosion initiation in reinforced concrete structures. *Mag Concrete Res* 55(2):117–124. doi:[10.1680/macrc.2003.55.2.117](https://doi.org/10.1680/macrc.2003.55.2.117)
42. Page CL, Page M (2007) *Durability of concrete and cement composites*. Woodhead Publishing Limited, Cambridge
43. Pedeferra P (1996) Cathodic protection and cathodic prevention. *Constr Build Mater* 10(5):391–402. doi:[10.1016/0950-0618\(95\)00017-8](https://doi.org/10.1016/0950-0618(95)00017-8)
44. Poupard O, L'Hostis V, Catinaud S, Petre-Lazar I (2006) Corrosion damage diagnosis of a reinforced concrete beam after 40 years natural exposure in marine environment. *Cement Concrete Res* 36(3):504–520. doi:[10.1016/j.cemconres.2005.11.004](https://doi.org/10.1016/j.cemconres.2005.11.004)
45. Pradhan B, Bhattacharjee B (2009) Half-cell potential as an indicator of chloride-induced rebar corrosion initiation in RC. *J Mater Civil Eng* 21(10):543–552. doi:[10.1061/ASCE0899-561200921:10543C](https://doi.org/10.1061/ASCE0899-561200921:10543C)
46. Pradhan B, Bhattacharjee B (2011) Rebar corrosion in chloride environment. *Constr Build Mater* 25(5):2565–2575. doi:[10.1016/j.conbuildmat.2010.11.099](https://doi.org/10.1016/j.conbuildmat.2010.11.099)
47. Ryou JS, Ann KY (2008) Variation in the chloride threshold level for steel corrosion in concrete arising from different chloride sources. *Mag Concrete Res* 60(3):177–187. doi:[10.1680/macrc.2008.60.3.177](https://doi.org/10.1680/macrc.2008.60.3.177)
48. Shi X, Xie N, Fortune K, Gong J (2012) Durability of steel reinforced concrete in chloride environments: an overview. *Constr Build Mater* 30:125–138. doi:[10.1016/j.conbuildmat.2011.12.038](https://doi.org/10.1016/j.conbuildmat.2011.12.038)
49. Song H-W, Jung M-S, Lee C-H, Kim S-H, Ann KY (2010) Influence of chemistry of chloride ions in cement matrix on corrosion of steel. *ACI Mater J* 107(4):332–339. doi:[10.14359/51663858](https://doi.org/10.14359/51663858)
50. Tang L, Utgenannt P (2009) A field study of critical chloride content in reinforced concrete with blended binder. *Mater Corros* 60(8):617–622. doi:[10.1002/maco.200905282](https://doi.org/10.1002/maco.200905282)
51. Taylor HFW (1990) *Cement chemistry*. Academic Press, London
52. Thomas M (1996) Chloride thresholds in marine concrete. *Cement Concrete Res* 26(4):513–519. doi:[10.1016/0008-8846\(96\)00035-X](https://doi.org/10.1016/0008-8846(96)00035-X)
53. Thomas MDA, Matthews JD (2004) Performance of pfa concrete in a marine environment: 10-year results. *Cement Concrete Comp* 26(1):5–20. doi:[10.1016/S0958-9465\(02\)00117-8](https://doi.org/10.1016/S0958-9465(02)00117-8)
54. Trejo D, Pillai RG (2003) Accelerated chloride threshold testing: part I—ASTM A 615 and A 706 Reinforcement. *ACI Mater J* 100(6):519–527. doi:[10.14359/12959](https://doi.org/10.14359/12959)
55. Tuutti K (1982) *Corrosion of steel in concrete*. Swedish foundation for concrete research, Stockholm
56. Xu J, Jiang L, Wang W, Xu Y, Jiang Y (2011) Chloride threshold value for reinforcement corrosion in concrete with additions of silica fume or fly ash. *Mag Concrete Res* 63(12):905–913. doi:[10.1680/macrc.10.00101](https://doi.org/10.1680/macrc.10.00101)
57. Yu H, Hartt H (2011) Correction of chloride threshold concentration and time-to-corrosion due to reinforcement presence. *Mater Corros* 62(5):423–430. doi:[10.1002/maco.200905516](https://doi.org/10.1002/maco.200905516)